

---

# Contrastive Learning for Unsupervised Domain Adaptation of Time Series

---

**Yilmazcan Ozyurt**  
ETH Zürich  
yozyurt@ethz.ch

**Stefan Feuerriegel**  
LMU Munich  
feuerriegel@lmu.de

**Ce Zhang**  
ETH Zürich  
ce.zhang@inf.ethz.ch

## Abstract

Unsupervised domain adaptation (UDA) aims at learning a machine learning model using a labeled source domain that performs well on a similar yet different, unlabeled target domain. UDA is important in many applications such as medicine, where it is used to adapt risk scores across different patient cohorts. In this paper, we develop a novel framework for UDA of time series data, called CLUDA. Specifically, we propose a contrastive learning framework to learn domain-invariant semantics in multivariate time series, so that these preserve label information for the prediction task. In our framework, we further capture semantic variation between source and target domain via nearest-neighbor contrastive learning. To the best of our knowledge, ours is the first framework to learn domain-invariant semantic information for UDA of time series data. We evaluate our framework using large-scale, real-world datasets with medical time series (i.e., MIMIC-IV and AmsterdamUMCdb) to demonstrate its effectiveness and show that it achieves state-of-the-art performance for time series UDA.

## 1 Introduction

Many real-world applications of machine learning are characterized by differences between the domains at training and at deployment [20, 23]. Therefore, effective methods are needed that learn domain-invariant representations across domains. For example, it is well known that medical settings suffer from substantial domain shifts due to differences in patient cohorts, medical routines, reporting practices, etc. [13, 44]. Hence, a machine learning model trained for one patient cohort may not generalize to other patient cohorts. Therefore, there is a great need for effective domain adaptation of time series.

Unsupervised domain adaptation (UDA) aims to learn a machine learning model using a labeled source domain that performs well on a similar yet different, unlabeled target domain [14, 25]. This setting is widespread in medical practice: before deployment, electronic health records provide direct access to unlabeled data for a new patient cohort or new health institution, i.e., for the new target domain, and thus to perform UDA.

So far, many methods for UDA have been proposed for computer vision [6, 14, 25, 30, 33, 34, 38, 39, 42, 45]. In contrast, comparatively few works have focused on UDA of time series. Here, previous works utilize a tailored feature extractor to capture temporal dynamics of multivariate time series, typically through recurrent neural networks (RNNs) [31], long short-term memory (LSTM) networks [4], and convolutional neural networks [24, 40, 41]. Some of these works minimize the domain discrepancy of learned features via adversarial-based methods [31, 40, 41] or restrictions through metric-based methods [4, 24]. However, to the best of our knowledge, there is no method for UDA of time series that captures and aligns the semantic information across source and target domain.

In this paper, we propose a novel framework for unsupervised domain adaptation of time series data based on contrastive learning, called CLUDA. Different from existing works, our CLUDA framework aims at capturing the semantic information in multivariate time series as a form of high-level features. To accomplish this, we incorporate the following components: (1) We minimize the domain discrepancy between source and target domains through adversarial training. (2) We capture the semantic information by generating positive pairs via a set of semantic-preserving augmentations and then learning their embeddings. For this, we make use of contrastive learning (CL). (3) We further capture the semantic variation between source and target domain via a custom nearest-neighborhood contrastive learning.

We evaluate our method on two large-scale, real-world datasets with medical time series, namely MIMIC-IV [21] and AmsterdamUMCdb [35]. We demonstrate the effectiveness of our framework for our medical setting and confirm its superior performance over state-of-the-art baselines. In fact, medical settings are known to suffer from substantial domain shifts (e. g., due to different patient cohorts, medical routines, reporting practices, etc., across health institutions) [13, 27, 44]. This highlights the relevance and practical need for adapting machine learning across domains from training and deployment.

### Contributions:<sup>1</sup>

1. We propose a novel, contrastive learning framework (CLUDA) for unsupervised domain adaptation of time series. To the best of our knowledge, ours is the first that learns domain-invariant semantics in multivariate time series to preserve information on labels.
2. We capture domain-invariant semantics in CLUDA through a custom approach combining nearest-neighborhood contrastive learning and adversarial learning to align them across domains.
3. We demonstrate the practical value of our framework using large-scale, real-world medical data from intensive care units. Thereby, we confirm that our CLUDA achieves state-of-the-art performance.

## 2 Related Work

**Contrastive learning:** Contrastive learning aims to learn representations with self-supervision, so that similar samples are embedded close to each other (positive pair) while pushing away samples that are dissimilar (negative pairs). Such representations have been shown to capture the semantic information of the samples by maximizing the lower bound of the mutual information between two augmented views [1, 36, 37].

Several methods for contrastive learning have been developed so far. For example, contrastive predictive coding (CPC) [28] predicts the next latent variable in contrast to negative samples from its proposal distribution. SimCLR stands for simple framework for CL of visual representations [7]. It maximizes the agreement between the embeddings of the two augmented views of the same sample and treat all the other samples in the same batch as negative samples. Nearest-neighbor CL (NNCL) [11] creates positive pairs from other samples in the dataset. For this, it takes the embedding of first augmented view and finds its nearest neighbor from the support set. Moment contrast (MoCo) [19] refers to the embeddings of two augmented views as query and key, and then constructs positive pairs for the sample as follows: Key embeddings are generated by a momentum encoder and stored in a queue (whose size is larger than the batch size), while all key embeddings are further used to construct negative pairs for the other sample. Thereby, MoCo generates more negative pairs than the batch size as compared to SimCLR, which is often more efficient in practice.

**Unsupervised domain adaptation:** Unsupervised domain adaptation leverages labeled source domain to predict the labels of a different, unlabeled target domain [14]. To achieve this, UDA methods typically aim to minimize the domain discrepancy and thereby decrease the lower bound of the target error [3]. To minimize the domain discrepancy, existing UDA methods can be loosely grouped into two categories: (1) *Adversarial-based methods* reduce the domain discrepancy via domain discriminator networks, which enforce the feature extractor to learn domain-invariant feature representations. Examples are domain adversarial neural network (DANN) [14], conditional domain adversarial

---

<sup>1</sup>Our code is available at <https://github.com/oezyurty/CLUDA>.

network (CDAN) [25], adversarial discriminative domain adaptation (ADDA) [39], multi-adversarial domain adaptation (MADA) [30], decision-boundary iterative refinement training with a teacher (DIRT-T) [33], and adversarial domain adaptation with domain mixup (DM-ADA) [42]. (2) *Metric-based methods* reduce the domain discrepancy by enforcing restrictions through a certain distance metric (e.g., via regularization). Examples are deep domain confusion (DDC) [38], correlation alignment via deep neural networks (Deep CORAL) [34], higher-order moment matching (HoMM) [6], and deep subdomain adaptation network (DSAN) [45].

However, previous works on UDA typically come from computer vision and, therefore, are not directly applicable to time series. In contrast, comparatively few works have been proposed for UDA of time series (see below). These works tailor their feature extractor to time series and minimize the domain discrepancy of learned features through adversarial learning or metric-based regularization, similar to UDA methods from computer vision.

**Unsupervised domain adaptation for time series:** A few methods have been tailored to unsupervised domain adaptation for time series data. Variational recurrent adversarial deep domain adaptation (VRADA) [31] was the first UDA method for multivariate time series that uses adversarial learning for reducing domain discrepancy. VRADA uses a variational recurrent neural network [10] as its feature extractor. Specifically, VRADA trains the classifier and the domain discriminator (adversarially) for the last latent variable of its variational recurrent neural network. Convolutional deep domain adaptation for time series (CoDATS) [40] builds upon the same adversarial training as VRADA, but uses convolutional neural network for the feature extractor instead. Time series sparse associative structure alignment (TS-SASA) [4] is a metric-based method. Here, intra-variables and inter-variables attention mechanism are aligned between the domains via the minimization of maximum mean discrepancy (MMD). Adversarial spectral kernel matching (AdvSKM) [24] is another metric-based method that aligns the two domains via MMD. Specifically, it introduces a spectral kernel mapping, from which the output is used to minimize MMD between the domains. Across all of the aforementioned methods, the aim is to align the features across source and target domain.

There are some extensions for specialized problems and are thus not applicable to our setting later. For instance, CALDA [41] is neural network similar to CoDATS but is tailored for multi-source domains. Because of this difference, this method is not applicable later as a baseline for our setting.

**Research gap:** For UDA of time series, existing works merely align the *features* across source and target domain. In contrast to that, we propose to align *semantic information* instead. To achieve this, we develop a novel framework called CLUDA based on contrastive learning.

### 3 Problem Definition

We consider a classification task for which we aim to perform unsupervised domain adaptation of time series. Specifically, we have two distributions over the time series from the source domain  $\mathcal{D}_S$  and the target domain  $\mathcal{D}_T$ . In our setup, we have **labeled** *i.i.d.* samples from the source domain given by  $\mathcal{S} = \{(x_i^s, y_i^s)\}_{i=1}^{N_s} \sim \mathcal{D}_S$ , where  $x_i^s$  is a sample of the source domain,  $y_i^s$  is the label for the given sample, and  $N_s$  is the overall number of *i.i.d.* samples from the source domain. In contrast, we have **unlabeled** *i.i.d.* samples from the target domain given by  $\mathcal{T} = \{x_i^t\}_{i=1}^{N_t} \sim \mathcal{D}_T$ , where  $x_i^t$  is a sample of the target domain and  $N_t$  is the overall number of *i.i.d.* samples from the target domain. For brevity, we omit the index  $i$  (i.e.,  $x^s$  instead of  $x_i^s$ ) when it is clear from the context.

In this paper, we specifically investigate the case of multivariate time series. Hence, each  $x_i$  (either from the source or target domain) is a sample of multivariate time series denoted by  $x_i = \{x_{it}\}_{t=1}^T \in \mathbb{R}^{M \times T}$ , where  $T$  is the number of time steps and  $x_{it} \in \mathbb{R}^M$  is  $M$  observations for the corresponding time step.

Our aim is to build a classifier that generalizes well over target samples  $\mathcal{T}$  by leveraging the labeled source samples  $\mathcal{S}$ . Importantly, labels for the target domain are **not** available during training. Instead, we later use the labeled target samples  $\mathcal{T}_{\text{test}} = \{(x_i^t, y_i^t)\}_{i=1}^{N_{\text{test}}} \sim \mathcal{D}_T$  only for the purpose of evaluating our framework.

The above setting is directly relevant for practice [13, 20, 23, 44]. For example, medical time series from different health institutions differ in terms of patient cohorts, medical routines, reporting practice, etc., and, therefore, are subject to substantial domain shifts. As such, data from training and data from deployment should be considered as different domains. Hence, in order to apply machine learning for

risk scoring or other medical use cases, it is important to adapt the machine learning model trained on one domain  $\mathcal{S}$  for another domain  $\mathcal{T}$  before deployment.

## 4 Proposed CLUDA Framework

In this section, we describe the components of our framework to learn domain-invariant semantic information of time series. We start with an overview of the neural architecture, and then describe how we (1) perform adversarial training, (2) align semantic information of domains, and (3) capture semantic variation across domains. The high-level overview of the neural architecture is shown in Fig. 1, and the complete CLUDA framework in Fig. 2.

### 4.1 Architecture

The neural architecture of our CLUDA for unsupervised domain adaptation of time series is shown in Fig. 1. Our architecture is informed by earlier works in adversarial domain adaptation [14]. Specifically, the components are as follows: (1) The **feature extractor** network  $F(\cdot)$  takes the original time series  $x^s$  and  $x^t$  from both domains and creates corresponding embeddings  $z^s$  and  $z^t$ , respectively. (2) The **classifier network**  $C(\cdot)$  is trained to predict the label  $y^s$  of time series from the source domain using the embeddings  $z^s$ . (3) The **discriminator network**  $D(\cdot)$  is trained to distinguish source embeddings  $z^s$  from target embeddings  $z^t$ . For such training, we introduce domain labels  $d = 0$  for source instances and  $d = 1$  for target instances.

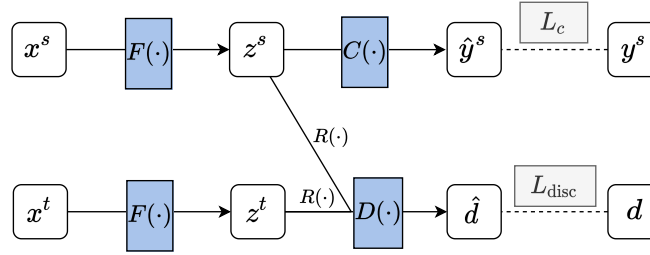


Figure 1: High-level overview of the neural architecture with adversarial domain adaptation.

### 4.2 Adversarial Training for Unsupervised Domain Adaptation

To train the above components, we minimize the combination of separate loss functions.

Our first loss,  $L_c$ , trains the feature extractor  $F(\cdot)$  and the classifier  $C(\cdot)$ . We train both jointly in order to correctly predict the labels from the source domain. For this, we define the prediction loss

$$L_c = \frac{1}{N_s} \sum_i^{N_s} L_{\text{pred}}(C(F(x_i^s)), y_i^s), \quad (1)$$

where  $L_{\text{pred}}(\cdot, \cdot)$  is cross-entropy loss.

Our second loss,  $L_{\text{disc}}$  is used to learn domain-invariant feature representations. Here, we use adversarial learning [14]. To this end, the domain discriminator  $D(\cdot)$  is trained to minimize the domain classification loss, whereas the feature extractor  $F(\cdot)$  is trained to maximize the same loss simultaneously. This is achieved by the gradient reversal layer  $R(\cdot)$  between  $F(\cdot)$  and  $D(\cdot)$ , defined by

$$R(x) = x, \quad \frac{dR}{dx} = -\mathbf{I}. \quad (2)$$

Hence, we yield the domain classification loss

$$L_{\text{disc}} = \frac{1}{N_s} \sum_i^{N_s} L_{\text{pred}}(D(R(F(x_i^s))), d_i^s) + \frac{1}{N_t} \sum_i^{N_t} L_{\text{pred}}(D(R(F(x_i^t))), d_i^t). \quad (3)$$

### 4.3 Aligning Semantic Information of Domains

In our CLUDA, we capture semantic information of time series in the embeddings  $z^s$  and  $z^t$ , and then align the semantic information of two domains for unsupervised domain adaptation. With this approach, we improve upon the earlier works in two ways: (1) We facilitate our feature extractor  $F(\cdot)$  to learn label-preserving information captured by the semantics. This observation was made earlier for unsupervised representation learning yet outside of our time series settings [1, 7, 8, 15, 17, 36, 37]. (2) We further hypothesize that discrepancy between the semantics of two domains is smaller than the discrepancy between their feature space, and therefore, the domain alignment task becomes easier.

To capture the semantics of time series for each domain, we leverage contrastive learning. CL is widely used in unsupervised representation learning for the downstream tasks in machine learning [7, 8, 19, 26, 43], while we adapt to learn semantic information. In plain words, CL approach aims to learn similar representations for two augmented views (positive pair) of the same sample in contrast to the views from other samples (negative pairs). This leads to a maximization of mutual information between two views and captures semantic information [1, 36, 37].

In our framework (see Fig. 2), we leverage contrastive learning in form of momentum contrast (MoCo) [19] in order to capture the semantic information from each domain. Accordingly, we apply semantic-preserving augmentations [9, 22, 43] to each sample of multivariate time series twice. Specifically, in our framework, we sequentially apply the following functions with random instantiations: history crop, history cutout, channel dropout, and Gaussian noise (see Appendix for details). After augmentation, we have two views of each sample, called query  $x_q$  and key  $x_k$ . These two views are then processed by the feature extractor to get their embeddings as  $z_q = F(x_q)$  and  $z_k = \tilde{F}(x_k)$ . Here,  $\tilde{F}(\cdot)$  is a *momentum-updated* feature extractor for MoCo.

To train the momentum-updated feature extractor, the gradients are not backpropagated through  $\tilde{F}(\cdot)$ . Instead, the weights  $\theta_{\tilde{F}}$  are updated by the momentum via

$$\theta_{\tilde{F}} \leftarrow m \theta_{\tilde{F}} + (1 - m) \theta_F, \quad (4)$$

where  $m \in [0, 1)$  is the momentum coefficient. The objective of MoCo-based contrastive learning is to project  $z_q$  via a projector network  $Q(\cdot)$  and bring the projection  $Q(z_q)$  closer to its positive sample  $z_k$  (as opposed to negative samples stored in queue  $\{z_{kj}\}_{j=1}^J$ ). After each training step, the batch of  $z_k$ 's are stored in queue of size  $J$ . As a result, for each domain we have the following contrastive loss

$$L_{CL} = -\frac{1}{N} \sum_{i=1}^N \log \frac{\exp(Q(z_{qi}) \cdot z_{ki}/\tau)}{\exp(Q(z_{qi}) \cdot z_{ki}/\tau) + \sum_{j=1}^J \exp(Q(z_{qi}) \cdot z_{kj}/\tau)}, \quad (5)$$

where  $\tau > 0$  is the temperature scaling parameter, and where all embeddings are normalized. Since we have two domains (i.e., source and target), we also have two contrastive loss components as  $L_{CL}^s$  and  $L_{CL}^t$  and two queues given by  $queue^s$  and  $queue^t$ .

For better readability, Fig. 2 shows the duplicated view of some network components for source and target samples. In fact, the weights of  $F(\cdot)$ ,  $\tilde{F}(\cdot)$ , and  $Q(\cdot)$  are shared across domains. We separately draw the discriminator  $D(\cdot)$  to avoid overlapping arrows in the figure.

### 4.4 Capturing Semantic Variation Across Domains

Our CLUDA framework further captures semantic variation across the source and target domain. To do so, we build upon ideas for nearest-neighbor contrastive learning [11] from unsupervised representation learning, yet outside of our time series setting. In the following, we develop a custom approach for nearest-neighbor contrastive learning for our time series setting. To the best of our knowledge, ours is the first nearest-neighbor contrastive learning approach for unsupervised domain adaptation of time series.

In our CLUDA framework, nearest-neighbor contrastive learning should facilitate the classifier  $C(\cdot)$  to make accurate predictions for the target domain. We achieve this by creating positive pairs between domains, whereby we explicitly align the semantics across domains. For this, we pair  $z_{qi}^t$  with the nearest-neighbor of  $z_{ki}^t$  from the source domain, denoted as  $NN_s(z_{ki}^t)$ . We thus introduce a corresponding loss

$$L_{NNCL} = -\frac{1}{N_t} \sum_{i=1}^{N_t} \log \frac{\exp(z_{qi}^t \cdot NN_s(z_{ki}^t)/\tau)}{\sum_{j=1}^{N_s} \exp(z_{qi}^t \cdot z_{qj}^s/\tau)}, \quad (6)$$

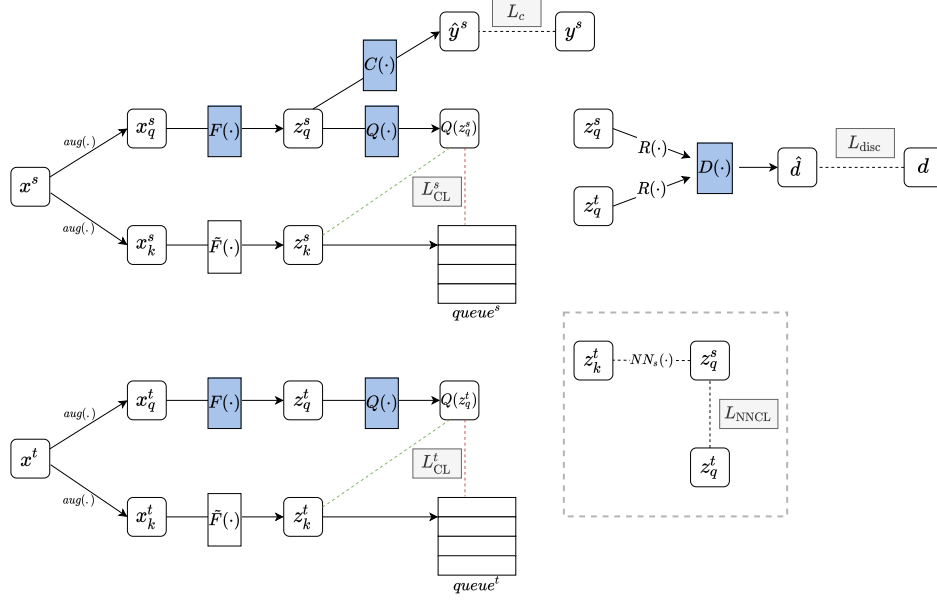


Figure 2: The complete CLUDA framework. The box dashed in gray shows the nearest-neighbor contrastive learning.

where  $NN_s(\cdot)$  retrieves the nearest-neighbor of an embedding from the source queries  $\{z_{qi}^s\}_{i=1}^{N_s}$ .

#### 4.5 Training

**Overall loss:** Overall, the CLUDA framework minimizes

$$L = L_c + \lambda_{\text{disc}} \cdot L_{\text{disc}} + \lambda_{\text{CL}} \cdot (L_{\text{CL}}^s + L_{\text{CL}}^t) + \lambda_{\text{NNCL}} \cdot L_{\text{NNCL}}, \quad (7)$$

where hyperparameters  $\lambda_{\text{disc}}$ ,  $\lambda_{\text{CL}}$ , and  $\lambda_{\text{NNCL}}$  control the contribution of the domain classification loss  $L_{\text{disc}}$ , the contrastive loss  $L_{\text{CL}}^s$  and  $L_{\text{CL}}^t$ , and nearest-neighbor contrastive loss  $L_{\text{NNCL}}$ , respectively.

**Implementation:** Our framework CLUDA (see Fig. 2) has multiple neural network components for end-to-end training of UDA for time series. We implement the feature extractor  $F(\cdot)$  via a temporal convolutional network (TCN) [2]. We use the convolutional kernel of size 3 and 64 filters. We stack 5 dilated convolutional layers for TCN so that receptive field covers the sufficient history of medical time series. We implement the discriminator  $D(\cdot)$ , the classifier  $C(\cdot)$ , and the projector  $Q(\cdot)$  via a multilayer perceptron with one hidden-layer. Details of architecture search for each component are given in Appendix.

## 5 Experimental Setup

To evaluate the effectiveness of our framework, we use real-world data from medicine. We intentionally chose this setting as medical applications are known to suffer from a substantial domain shifts (e. g., due to different patient cohorts, medical routines, reporting practices, etc., across health institutions) [13, 27, 44]. We then predict health outcomes analogous to earlier works [4, 5, 16, 29, 31].

**Datasets:** We use **MIMIC-IV** [21] and **AmsterdamUMCdb (AUMC)** [35]. Both are de-identified, publicly-available data from intensive care unit stays, where the goal is to predict different health outcomes of inpatients (e.g., mortality). To date, MIMIC-IV is the largest public dataset for intensive care units with 49,351 ICU stays; AmsterdamUMCdb contains 19,840 ICU stays. However, both have a different origin (Boston, United States vs. Amsterdam, Netherlands) and thus reflect patients with different characteristics, medical procedures, etc. Table 1 shows summary statistics from each dataset. Additional details on the datasets are in the Appendix.

Table 1: Summary of datasets.

Name	From	#Patients	#Measurements	Avg. ICU stay (hours)	Mortality (%)
MIMIC	US	49,351	41	72.21	9.95
AUMC	Europe	19,840	41	100.13	8.62

**Tasks:** We compare the performance of our framework across 3 different standard tasks from the literature [4, 5, 16, 18, 29, 31, 32]. (1) *Decompensation* prediction refers to predicting whether the patient dies within the next 24 hours. (2) *Mortality* prediction refers to predicting whether the patient dies during his/her ICU stay. (3) *Length of stay* prediction refers to predicting the remaining hours of ICU stay for the given patient. This serves as a proxy of the overall health outcome. The distribution of remaining length of ICU stay contains a heavy tail (see Appendix), which makes it challenging to model it as a regression task. Therefore, we follow the previous works [18, 32] and divide the range of values into 10 buckets and perform an ordinal multiclass classification.

For each task, we performed unsupervised domain adaptation in both ways: MIMIC (source)  $\mapsto$  AUMC (target), and AUMC (source)  $\mapsto$  MIMIC (target). Later, we also report the corresponding performance on the test samples from the source dataset (i.e., MIMIC  $\mapsto$  MIMIC, and AUMC  $\mapsto$  AUMC). This way, we aim to provide insights to what extent the different UDA methods provide a trade-off for the performance in the source vs. target domain. It also be loosely interpreted as a upper bound for the prediction performance.

**Performance metrics:** We report the following performance metrics. The tasks for predicting (1) *decompensation* and (2) *mortality* are binary classification problems. For these tasks, we compare the area under the receiver operating characteristics curve (AUROC) and area under the precision-recall curve (AUPRC). Results for AUPRC are in the Appendix due to space limitation. The task of predicting (3) *length of stay* is an ordinal multiclass classification problem. For this, we report Cohen’s linear weighted kappa, which measures the correlation between the predicted and ground-truth classes.

**Baselines:** We compare the performance of our framework against several baselines. (1) We report the performance of a model without UDA (**w/o UDA**) to show the overall contribution of UDA methods. For this, we only use feature extractor  $F(\cdot)$  and the classifier  $C(\cdot)$  using the same architecture as in our CLUDA. This model is only trained on source domain and tested on both domains when reporting the results. (2) We implement the following state-of-the-art baselines for UDA of time series data. These are: **VRADA** [31], **CoDATS** [40], **TS-SASA** [4], and **AdvSKM** [24]. In our results later, we do not list TS-SASA as it repeatedly did not perform better than random for our experiments and was thus discarded for reasons of space. Of note, we also do not report results for CALDA [41] as it aims at a different setting (multi-source domain) and is thus not applicable to ours. (3) We additionally implement **CDAN** [25]. CDAN was originally developed for computer vision, and we thus tailor its feature extractor to time series through temporal convolutional network.

**Pre-processing:** We split the patients of each dataset into 3 parts for training/validation/testing (ratio: 70/15/15). We used a stratified split based on the mortality label. We proceeded analogous to previous works for pre-processing [18, 32]. Each measurement was sampled to hourly resolution, and missing measurements were filled with forward-filling imputation. We applied standard scaling to each measurement based on the statistics from training set. The remaining missing measurements were filled with zero, which corresponds to mean imputation after scaling. We followed best practices in benchmarking data from intensive care units [18, 32]. That is, for each of the tasks, we start making the prediction at four hours after the ICU admission. In all our experiments, we used a maximum history length  $T = 48$  hours. Shorter sequences were pre-padded by zero.

**Training:** We used the Adam optimizer with a learning rate varying between  $5 \cdot 10^{-5}$  and  $5 \cdot 10^{-4}$  as a hyperparameter. We trained all models for 20K steps with batch size of 2048 (except AdvSKM with a batch size of 1024 to fit into GPU). We applied early stopping based on the performance of validation set without the labels from target domain. We tuned the hyperparameters based on validation performance via grid search. We trained and tested all models on NVIDIA GeForce GTX 1080 Ti with 11GB GPU memory. The rest of the implementation details (incl. runtime details) are in the Appendix.

Table 2: Decompensation prediction. Shown: AUROC (*mean*  $\pm$  *std*) over 10 random initializations.

Source	MIMIC		AUMC	
Target	MIMIC	AUMC	AUMC	MIMIC
w/o UDA	0.831 $\pm$ 0.001	0.771 $\pm$ 0.004	0.813 $\pm$ 0.005	0.745 $\pm$ 0.004
VRADA[31]	0.817 $\pm$ 0.002	0.773 $\pm$ 0.003	0.798 $\pm$ 0.003	0.764 $\pm$ 0.002
CoDATS[40]	0.825 $\pm$ 0.003	0.772 $\pm$ 0.004	0.818 $\pm$ 0.005	0.762 $\pm$ 0.002
AdvSKM[24]	0.824 $\pm$ 0.002	0.775 $\pm$ 0.003	0.817 $\pm$ 0.004	0.766 $\pm$ 0.001
CDAN[25]	0.824 $\pm$ 0.001	0.768 $\pm$ 0.003	0.817 $\pm$ 0.005	0.763 $\pm$ 0.005
CLUDA (ours)	0.832 $\pm$ 0.002	<b>0.791 <math>\pm</math> 0.004</b>	<b>0.825 <math>\pm</math> 0.001</b>	<b>0.774 <math>\pm</math> 0.002</b>

Higher is better. Best value in bold. Black font: main results for UDA. Gray font: source  $\mapsto$  source.

Table 3: In-hospital mortality prediction. Shown: AUROC (*mean*  $\pm$  *std*) over 10 random initializations.

Source	MIMIC		AUMC	
Target	MIMIC	AUMC	AUMC	MIMIC
w/o UDA	0.831 $\pm$ 0.001	0.709 $\pm$ 0.002	0.721 $\pm$ 0.005	0.774 $\pm$ 0.006
VRADA[31]	0.827 $\pm$ 0.001	0.726 $\pm$ 0.005	0.729 $\pm$ 0.006	0.778 $\pm$ 0.002
CoDATS[40]	0.832 $\pm$ 0.001	0.708 $\pm$ 0.005	0.724 $\pm$ 0.004	0.778 $\pm$ 0.004
AdvSKM[24]	0.830 $\pm$ 0.001	0.707 $\pm$ 0.001	0.724 $\pm$ 0.005	0.772 $\pm$ 0.004
CDAN[25]	0.776 $\pm$ 0.001	0.716 $\pm$ 0.006	0.712 $\pm$ 0.004	0.772 $\pm$ 0.003
CLUDA (ours)	0.836 $\pm$ 0.001	<b>0.739 <math>\pm</math> 0.004</b>	<b>0.750 <math>\pm</math> 0.001</b>	<b>0.789 <math>\pm</math> 0.002</b>

Higher is better. Best value in bold. Black font: main results for UDA. Gray font: source  $\mapsto$  source.

## 6 Results

### 6.1 Prediction Performance

We now demonstrate that our CLUDA framework achieves the state-of-the-art performance across all UDA tasks. The results compare the tasks of predicting decompensation (Table 2), mortality (Table 3), and length of stay (Table 4). Therein, the UDA results are in black font.

**Source  $\mapsto$  target:** For all tasks, our CLUDA framework consistently improves UDA performance for both target domains. For the decompensation prediction, our framework yields an improvement over the best UDA baseline by 2.1 % (MIMIC  $\mapsto$  AUMC) and 1.0 % (AUMC  $\mapsto$  MIMIC). For the mortality prediction, our framework outperforms the best UDA baseline by 1.8 % (MIMIC  $\mapsto$  AUMC) and 1.4 % (AUMC  $\mapsto$  MIMIC). For length of stay prediction, our framework achieves an improvement over the best UDA baseline by 17.4 % (MIMIC  $\mapsto$  AUMC) and 0.2 % (AUMC  $\mapsto$  MIMIC).

We further compare the performance gap between (1) the baseline with no domain adaptation (w/o UDA) vs. (2) the source  $\mapsto$  source setting, and thereby examine to what extent our CLUDA can close this performance gap. Here, we interpret (2) as a loose upper bound. For instance, in decompensation prediction for AUMC, our CLUDA (0.791 AUROC) fills 47.6 % of the performance gap between MIMIC  $\mapsto$  AUMC (0.771 AUROC) and AUMC  $\mapsto$  AUMC (0.813 AUROC) of w/o UDA. In contrast, the best baseline model of this task (AdvSKM) can only fill 9.5 % of the same performance gap (0.775 AUROC). Altogether, this demonstrates the effectiveness of our proposed framework.

**Source  $\mapsto$  source:** As an additional check, we also report the performance of all methods for the source  $\mapsto$  source setting in order to assess how robust the performance remains. That is, we report the performance for test samples from source domain. This is shown in gray color in Tables 2 to 4. Importantly, we do not see a drop in performance, and, therefore, the performance remains robust. On the contrary, we observe that the UDA methods can actually improve the performance on the labeled source dataset by leveraging the unlabeled dataset. This suggests that UDA methods may even serve as data augmentation.

### 6.2 Ablation Study

We conduct an ablation study (see Table 5) to better understand the importance of the different components in our framework. For this, we deactivated some of the components and thus yield 5



Table 4: Length of stay prediction. Shown: KAPPA (*mean*  $\pm$  *std*) over 10 random initializations.

Source	MIMIC		AUMC	
Target	MIMIC	AUMC	AUMC	MIMIC
w/o UDA	0.178 $\pm$ 0.002	0.169 $\pm$ 0.003	0.246 $\pm$ 0.001	0.122 $\pm$ 0.001
VRADA[31]	0.168 $\pm$ 0.003	0.161 $\pm$ 0.007	0.241 $\pm$ 0.002	0.126 $\pm$ 0.004
CoDATS[40]	0.174 $\pm$ 0.002	0.159 $\pm$ 0.002	0.243 $\pm$ 0.001	0.120 $\pm$ 0.003
AdvSKM[24]	0.179 $\pm$ 0.002	0.172 $\pm$ 0.005	0.244 $\pm$ 0.002	0.123 $\pm$ 0.004
CDAN[25]	0.176 $\pm$ 0.002	0.138 $\pm$ 0.004	0.244 $\pm$ 0.002	0.124 $\pm$ 0.002
CLUDA (ours)	<b>0.216 <math>\pm</math> 0.001</b>	<b>0.202 <math>\pm</math> 0.006</b>	<b>0.276 <math>\pm</math> 0.002</b>	<b>0.129 <math>\pm</math> 0.003</b>

Higher is better. Best value in bold. Black font: main results for UDA. Gray font: source  $\mapsto$  source.

Table 5: Ablation study for decompensation prediction. Shown: AUROC (*mean*  $\pm$  *std*) over 10 random initializations.

Source	MIMIC	
Target	MIMIC	AUMC
w/o UDA	0.831 $\pm$ 0.001	0.771 $\pm$ 0.004
w/o CL and w/o NNCL ( $\lambda_{CL} = 0, \lambda_{NNCL} = 0$ )	0.825 $\pm$ 0.003	0.772 $\pm$ 0.004
w/o CL ( $\lambda_{CL} = 0$ )	0.833 $\pm$ 0.002	0.782 $\pm$ 0.003
w/o NNCL ( $\lambda_{NNCL} = 0$ )	0.833 $\pm$ 0.001	0.786 $\pm$ 0.003
w/o Discriminator ( $\lambda_{disc} = 0$ )	<b>0.841 <math>\pm</math> 0.001</b>	0.787 $\pm$ 0.003
CLUDA (ours)	0.832 $\pm$ 0.002	<b>0.791 <math>\pm</math> 0.004</b>

Higher is better. Best value in bold. Black font: main results for UDA. Gray font: source  $\mapsto$  source.

different variants of our CLUDA. We then re-ran the experiments for decompensation prediction task. Additional results are in the Appendix.

We compare the following variants: (1) We again report the **w/o UDA** baseline from above for a better comparison. This is inferior to our CLUDA and, as expected, has the lowest performance of all variants. (2) **w/o CL and w/o NNCL** refers to a base architecture from Sec. 4.2. It includes adversarial training but without aligning semantic information and without capturing semantic variation. This shows that the combination of CL and NNCL is important for the performance of our framework. We now assess their relative contribution. (3) **w/o CL** deactivates contrastive learning for aligning semantic information across source and target domains. (4) **w/o NNCL** deactivates the nearest-neighbor contrastive learning for capturing semantic variation across source and target domain. Overall, the drop in performance is larger for CL than for NNCL, implying the importance of aligning semantic information for our framework. (5) **w/o Discriminator** deactivates the discriminator. Evidently, the discriminator facilitates better UDA for the target domain but only to smaller extent than the other components. We further observe a better performance in the source domain without the discriminator. This implies that the discriminator leads to loss in preserving label information for the source domain and, in return, facilitates a better generalization over the target domain. (6) Our CLUDA works overall best on the target domain, thereby justifying our chosen architecture.

## 7 Conclusion

In this paper, we propose a novel framework for unsupervised domain adaptation (UDA) of time series based on contrastive learning, called CLUDA. To the best of our knowledge, CLUDA is the first approach that learns domain-invariant semantics in multivariate time series for UDA. As shown in our experiments with real-world, medical data, CLUDA achieves state-of-the-art performance for UDA of time series.

We expect our framework of direct relevance for medical applications where risk scores should be transferred across populations or institutions, thereby providing social value through a further personalization of care. Thereby, we fulfill a direct need in medical practice raised only recently [12]. As with all real-world application in medicine, we usher for a careful use to ensure safe and reliable applications.

## References

- [1] Philip Bachman, R Devon Hjelm, and William Buchwalter. Learning representations by maximizing mutual information across views. *NeurIPS*, 2019.
- [2] Shaojie Bai, J Zico Kolter, and Vladlen Koltun. An empirical evaluation of generic convolutional and recurrent networks for sequence modeling. *arXiv preprint arXiv:1803.01271*, 2018.
- [3] Shai Ben-David, John Blitzer, Koby Crammer, Alex Kulesza, Fernando Pereira, and Jennifer Wortman Vaughan. A theory of learning from different domains. *JMLR*, 79:151–175, 2010.
- [4] Ruichu Cai, Jiawei Chen, Zijian Li, Wei Chen, Keli Zhang, Junjian Ye, Zhuozhang Li, Xiaoyan Yang, and Zhenjie Zhang. Time series domain adaptation via sparse associative structure alignment. In *AAAI*, 2021.
- [5] Zhengping Che, Sanjay Purushotham, Kyunghyun Cho, David Sontag, and Yan Liu. Recurrent neural networks for multivariate time series with missing values. *Scientific Reports*, 2018.
- [6] Chao Chen, Zhihang Fu, Zhihong Chen, Sheng Jin, Zhaowei Cheng, Xinyu Jin, and Xian-Sheng Hua. Homm: Higher-order moment matching for unsupervised domain adaptation. In *AAAI*, 2020.
- [7] Ting Chen, Simon Kornblith, Mohammad Norouzi, and Geoffrey Hinton. A simple framework for contrastive learning of visual representations. In *ICML*, 2020.
- [8] Xinlei Chen, Haoqi Fan, Ross Girshick, and Kaiming He. Improved baselines with momentum contrastive learning. *arXiv preprint arXiv:2003.04297*, 2020.
- [9] Joseph Y Cheng, Hanlin Goh, Kaan Dogrusoz, Oncel Tuzel, and Erdrin Azemi. Subject-aware contrastive learning for biosignals. *arXiv preprint arXiv:2007.04871*, 2020.
- [10] Junyoung Chung, Kyle Kastner, Laurent Dinh, Kratarth Goel, Aaron C Courville, and Yoshua Bengio. A recurrent latent variable model for sequential data. *NeurIPS*, 2015.
- [11] Debidatta Dwibedi, Yusuf Aytar, Jonathan Tompson, Pierre Sermanet, and Andrew Zisserman. With a little help from my friends: Nearest-neighbor contrastive learning of visual representations. In *ICCV*, 2021.
- [12] Samuel G Finlayson, Adarsh Subbaswamy, Karandeep Singh, John Bowers, Annabel Kupke, Jonathan Zittrain, Isaac S Kohane, and Suchi Saria. The clinician and dataset shift in artificial intelligence. *NEJM*, 385(3), 2021.
- [13] Joseph Futoma, Morgan Simons, Trishan Panch, Finale Doshi-Velez, and Leo Anthony Celi. The myth of generalisability in clinical research and machine learning in health care. *The Lancet Digital Health*, 2(9), 2020.
- [14] Yaroslav Ganin, Evgeniya Ustinova, Hana Ajakan, Pascal Germain, Hugo Larochelle, François Laviolette, Mario Marchand, and Victor Lempitsky. Domain-adversarial training of neural networks. *JMLR*, 17: 2096–2030, 2016.
- [15] Songwei Ge, Shlok Mishra, Chun-Liang Li, Haohan Wang, and David Jacobs. Robust contrastive learning using negative samples with diminished semantics. *NeurIPS*, 2021.
- [16] Wendong Ge, Jin-Won Huh, Yu Rang Park, Jae-Ho Lee, Young-Hak Kim, and Alexander Turchin. An interpretable icu mortality prediction model based on logistic regression and recurrent neural networks with lstm units. In *AMIA Annual Symposium Proceedings*, 2018.
- [17] Jean-Bastien Grill, Florian Strub, Florent Altché, Corentin Tallec, Pierre Richemond, Elena Buchatskaya, Carl Doersch, Bernardo Avila Pires, Zhaohan Guo, Mohammad Gheshlaghi Azar, et al. Bootstrap your own latent-a new approach to self-supervised learning. *NeurIPS*, 2020.
- [18] Hrayr Harutyunyan, Hrant Khachatrian, David C Kale, Greg Ver Steeg, and Aram Galstyan. Multitask learning and benchmarking with clinical time series data. *Scientific Data*, 2019.
- [19] Kaiming He, Haoqi Fan, Yuxin Wu, Saining Xie, and Ross Girshick. Momentum contrast for unsupervised visual representation learning. In *CVPR*, 2020.
- [20] Dan Hendrycks and Thomas Dietterich. Benchmarking neural network robustness to common corruptions and perturbations. In *ICLR*, 2019.
- [21] Alistair Johnson, Lucas Bulgarelli, Tom Pollard, Steven Horng, Leo Anthony Celi, and R Mark IV. MIMIC-IV. *PhysioNet*, 2020.

- [22] Dani Kiyasseh, Tingting Zhu, and David A Clifton. Clocs: contrastive learning of cardiac signals across space, time, and patients. In *ICML*, 2021.
- [23] Pang Wei Koh, Shiori Sagawa, Henrik Marklund, Sang Michael Xie, Marvin Zhang, Akshay Balsubramani, Weihua Hu, Michihiro Yasunaga, Richard Lanus Phillips, Irena Gao, et al. Wilds: A benchmark of in-the-wild distribution shifts. In *ICML*, 2021.
- [24] Qiao Liu and Hui Xue. Adversarial spectral kernel matching for unsupervised time series domain adaptation. In *IJCAI*, 2021.
- [25] Mingsheng Long, Zhangjie Cao, Jianmin Wang, and Michael I Jordan. Conditional adversarial domain adaptation. *NeurIPS*, 2018.
- [26] Mostafa Neo Mohsenvand, Mohammad Rasool Izadi, and Pattie Maes. Contrastive representation learning for electroencephalogram classification. In *Machine Learning for Healthcare*. PMLR, 2020.
- [27] Bret Nestor, Matthew BA McDermott, Willie Boag, Gabriela Berner, Tristan Naumann, Michael C Hughes, Anna Goldenberg, and Marzyeh Ghassemi. Feature robustness in non-stationary health records: caveats to deployable model performance in common clinical machine learning tasks. In *Machine Learning for Healthcare*. PMLR, 2019.
- [28] Aaron van den Oord, Yazhe Li, and Oriol Vinyals. Representation learning with contrastive predictive coding. *arXiv preprint arXiv:1807.03748*, 2018.
- [29] Yilmazcan Ozyurt, Mathias Kraus, Tobias Hatt, and Stefan Feuerriegel. Attdmm: an attentive deep markov model for risk scoring in intensive care units. In *KDD*, 2021.
- [30] Zhongyi Pei, Zhangjie Cao, Mingsheng Long, and Jianmin Wang. Multi-adversarial domain adaptation. In *AAAI*, 2018.
- [31] Sanjay Purushotham, Wilka Carvalho, Tanachat Nilanon, and Yan Liu. Variational recurrent adversarial deep domain adaptation. In *ICLR*, 2017.
- [32] Sanjay Purushotham, Chuizheng Meng, Zhengping Che, and Yan Liu. Benchmarking deep learning models on large healthcare datasets. *Journal of Biomedical Informatics*, 2018.
- [33] Rui Shu, Hung H Bui, Hirokazu Narui, and Stefano Ermon. A dirt-t approach to unsupervised domain adaptation. In *ICLR*, 2018.
- [34] Baochen Sun and Kate Saenko. Deep coral: Correlation alignment for deep domain adaptation. In *ECCV*, 2016.
- [35] Patrick J Thorat, Jan M Peppink, Ronald H Driessen, Eric JG Sijbrands, Erwin JO Kompanje, Lewis Kaplan, Heatherlee Bailey, Jozef Kesecioglu, Maurizio Cecconi, Matthew Churpek, et al. Sharing icu patient data responsibly under the society of critical care medicine/european society of intensive care medicine joint data science collaboration: the amsterdam university medical centers database (amsterdamumcdb) example. *Critical Care Medicine*, 2021.
- [36] Yonglong Tian, Dilip Krishnan, and Phillip Isola. Contrastive multiview coding. In *ECCV*, 2020.
- [37] Yonglong Tian, Chen Sun, Ben Poole, Dilip Krishnan, Cordelia Schmid, and Phillip Isola. What makes for good views for contrastive learning? *NeurIPS*, 2020.
- [38] Eric Tzeng, Judy Hoffman, Ning Zhang, Kate Saenko, and Trevor Darrell. Deep domain confusion: Maximizing for domain invariance. *arXiv preprint arXiv:1412.3474*, 2014.
- [39] Eric Tzeng, Judy Hoffman, Kate Saenko, and Trevor Darrell. Adversarial discriminative domain adaptation. In *CVPR*, 2017.
- [40] Garrett Wilson, Janardhan Rao Doppa, and Diane J Cook. Multi-source deep domain adaptation with weak supervision for time-series sensor data. In *KDD*, 2020.
- [41] Garrett Wilson, Janardhan Rao Doppa, and Diane J Cook. Calda: Improving multi-source time series domain adaptation with contrastive adversarial learning. *arXiv preprint arXiv:2109.14778*, 2021.
- [42] Minghao Xu, Jian Zhang, Bingbing Ni, Teng Li, Chengjie Wang, Qi Tian, and Wenjun Zhang. Adversarial domain adaptation with domain mixup. In *AAAI*, 2020.
- [43] Hugo Yèche, Gideon Dresdner, Francesco Locatello, Matthias Hüser, and Gunnar Rätsch. Neighborhood contrastive learning applied to online patient monitoring. In *ICML*, 2021.

- [44] John R Zech, Marcus A Badgeley, Manway Liu, Anthony B Costa, Joseph J Titano, and Eric Karl Oermann. Variable generalization performance of a deep learning model to detect pneumonia in chest radiographs: a cross-sectional study. *PLoS Medicine*, 15(11), 2018.
- [45] Yongchun Zhu, Fuzhen Zhuang, Jindong Wang, Guolin Ke, Jingwu Chen, Jiang Bian, Hui Xiong, and Qing He. Deep subdomain adaptation network for image classification. *IEEE Transactions on Neural Networks and Learning Systems*, 2020.

## A Dataset Details

Table 6 provides additional details for both datasets MIMIC and AUMC. Both comprise of 41 separate time series, which are then used to predict the outcomes of interest – i.e., decompensation, in-hospital mortality and length of stay – via unsupervised domain adaptation.

Table 6: Descriptions of medical time series and their summary statistics for MIMIC and AUMC

Measurement	Unit	MIMIC		AUMC	
		Mean	Std. Dev.	Mean	Std. Dev.
Albumin	g/dL	3.053	0.697	2.121	0.575
Alkaline phosphatase	IU/L	115.384	36.044	146.459	49.948
Alanine aminotransferase	IU/L	110.340	98.699	100.352	89.697
Aspartate aminotransferase	IU/L	142.194	160.053	115.663	131.497
Base excess	mEq/L	0.691	1.744	1.291	1.740
Bicarbonate	mEq/L	24.613	4.815	25.815	4.753
Total bilirubin	mg/dL	2.060	4.815	0.975	2.081
Blood urea nitrogen	mg/dL	28.063	23.073	33.112	24.829
Calcium	mg/dL	8.398	0.746	8.121	0.773
Calcium ionized	mmol/L	1.126	0.086	1.161	0.094
Creatine kinase	IU/L	978.735	1402.472	755.806	1163.575
Chloride	mEq/L	103.881	6.224	107.083	6.796
Creatinine	mg/dL	1.364	1.336	1.214	1.001
Diastolic blood pressure	mmHg	63.513	14.857	62.199	14.037
Endtidal co2	mmHg	35.861	7.658	35.405	8.044
Fraction of inspired oxygen	%	48.213	15.95	43.345	10.106
Glucose	mg/dL	134.981	50.227	134.112	36.688
Hematocrit	%	30.850	5.736	31.108	5.230
Hemoglobin	g/dL	10.178	1.983	10.354	1.740
Heart rate	bpm	85.249	17.935	86.609	18.858
Prothrombin time/inter. norm. ratio	–	1.381	0.616	1.312	0.476
Potassium	mEq/L	4.088	0.552	4.141	0.453
Lactate	mmol/L	1.685	1.207	1.674	1.388
Mean arterial pressure	mmHg	79.481	15.368	84.444	17.149
Magnesium	mg/dL	2.107	0.347	2.160	0.446
Sodium	mEq/L	139.079	5.037	140.119	5.324
Co2 partial pressure	mmHg	41.259	9.551	41.590	8.355
Ph of blood	–	7.401	0.070	7.411	0.069
Phosphate	mg/dL	3.503	1.290	3.514	1.240
Platelet count	K/uL	213.982	127.242	245.261	160.271
O2 partial pressure	mmHg	114.686	62.778	101.140	34.704
Partial thromboplastin time	sec	36.537	18.426	44.364	18.862
Systolic blood pressure	mmHg	121.044	21.61	130.308	27.870
Temperature	C	36.949	0.634	36.600	1.095
White blood cell count	K/uL	12.152	8.583	13.314	7.804
Basophils	%	0.264	0.362	0.227	0.417
Eosinophils	%	1.208	1.996	1.167	1.716
Lymphocytes	%	12.316	10.53	11.311	9.873
Neutrophils	%	78.296	13.358	77.720	12.778
Prothrombine time	sec	15.141	6.262	3.455	43.459
Red blood cell count	m/uL	3.398	0.684	3.578	0.886

Table 7 shows the number of patients and the number of samples for each split and each dataset. As a reminder, since we start making the prediction at four hours after the ICU admission, the same patient yields multiple samples when training/testing the models.

Table 7: Number of patients and samples for each dataset and each split

	MIMIC			AUMC		
	Train	Validation	Test	Train	Validation	Test
Number of patients	34,290	7,343	7,353	13,802	2958	2964
Number of samples	2,398,546	513,636	512,454	1,332,390	304,981	287,599

### Summary statistics for “length of stay”

Here, we provide additional summary statistics for the distribution of “length of stay”. Figure 3 and Figure 4 show the length of stay distribution of all patients in the MIMIC and AUMC datasets, respectively. Further, Figure 5 and Figure 6 show the remaining length of stay distribution for all samples (i.e., all time windows considered for all patients) in MIMIC and AUMC, respectively. Recall that we divide the values of remaining length of stay into 10 buckets; the corresponding fraction of samples belonging to each bucket is reported in Figure 7.

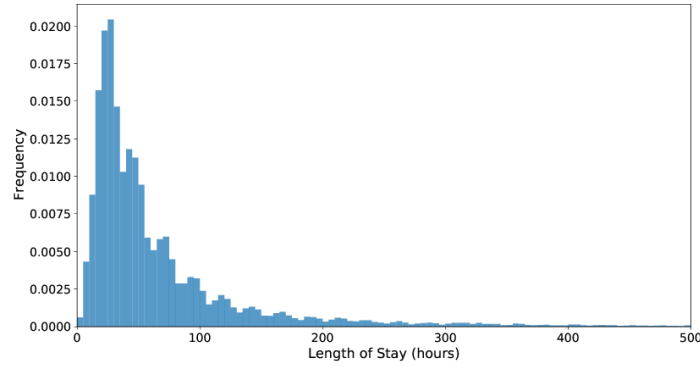


Figure 3: Length of stay distribution of MIMIC patients. For reasons of space, the distribution is cropped at a value of 500.

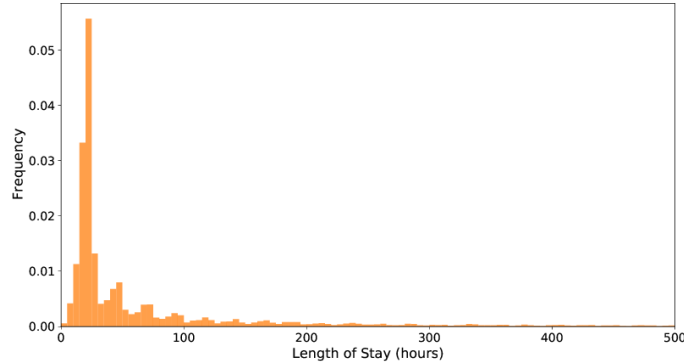


Figure 4: Length of stay distribution of AUMC patients. For reasons of space, the distribution is cropped at a value of 500.

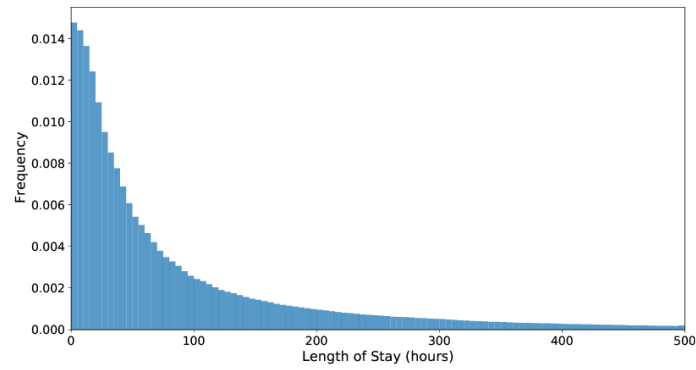


Figure 5: Remaining length of stay distribution of all MIMIC samples. For reasons of space, the distribution is cropped at a value of 500.

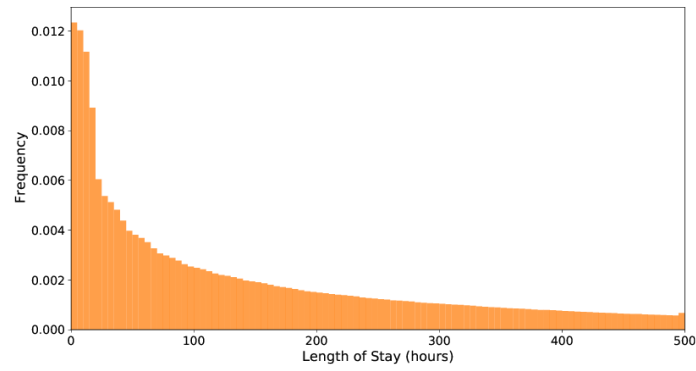


Figure 6: Remaining length of stay distribution of all AUMC samples. TFor reasons of space, the distribution is cropped at a value of 500.

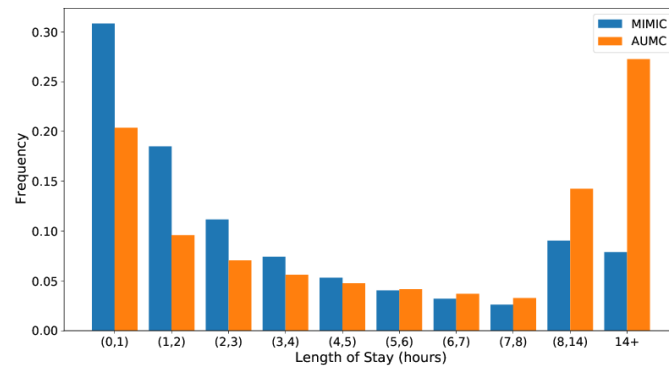


Figure 7: Histogram showing the distribution of remaining length of stay (MIMIC vs. AUMC). The buckets are the following: one bucket for less than one day, one bucket each for days 1 through 7, one bucket for the interval between 7 and 14 days, and one bucket for more than 14 days.

## B Training Details

In this section, we provide details on the hyperparameters tuning. Table 8 lists the tuning range of all hyperparameters. To avoid repetition, we list hyperparameters that appear at all methods in the first rows of Table 8. For each task (i. e., decompensation, in-hospital mortality, and length of stay prediction), we performed a grid search for hyperparameter tuning *separately* for each method.

Table 8: Hyperparameter tuning.

Method	Hyperparameter	Tuning Range
All methods, w/o UDA	Classifier hidden dim.	64, 128, 256
	Batch normalization	True, False
	Dropout	0, 0.1, 0.2
	Learning rate	$5 \cdot 10^{-5}$ , $2 \cdot 10^{-4}$ , $5 \cdot 10^{-4}$
	Weight decay	$1 \cdot 10^{-4}$ , $1 \cdot 10^{-3}$ , $1 \cdot 10^{-4}$
VRADA[31]	VRNN hidden dim.	32, 62, 128
	VRNN latent dim.	32, 64, 128
	VRNN num. layers	1, 2, 3
	Discriminator hidden dim.	64, 128, 256
	Weight discriminator loss	0.1, 0.5, 1
	Weight KL divergence	0.1, 0.5, 1
	Weight neg. log-likelihood	0.1, 0.5, 1
CoDATS[40]	Discriminator hidden dim.	64, 128, 256
	Weight discriminator loss	0.1, 0.5, 1
TS-SASA[4]	LSTM hidden dim	4, 8, 12
	Num. segments	4, 8, 12, 24
	Segment lengths	3, 6, 12, 24
	MMD kernel type	Linear, Gaussian
	Weight intra-attention loss	0.1, 0.5, 1
	Weight inter-attention loss	0.1, 0.5, 1
AdvSKM[24]	Spectral kernel hidden dim.	32, 64, 128
	Spectral kernel output dim.	32, 64, 128
	Spectral kernel type	Linear, Gaussian
	Num. kernel (if Gaussian)	3, 5, 7
	Weight MMD loss	0.1, 0.5, 1
CDAN[25]	Discriminator hidden dim.	64, 128, 256
	Multiplier discriminator update	0.1, 1, 10
	Weight discriminator loss	0.1, 0.5, 1
	Weight conditional entropy loss	0.1, 0.5, 1
CLUDA (ours)	Momentum	0.9, 0.95, 0.99
	Queue size	24576, 49152, 98304
	Discriminator hidden dim.	64, 128, 256
	Projector hidden dim.	64, 128, 256
	$\lambda_{\text{disc}}$	0.1, 0.5, 1
	$\lambda_{\text{CL}}$	0.05, 0.1, 0.2
	$\lambda_{\text{NNCL}}$	0.05, 0.1, 0.2

We implemented our CLUDA framework and all the baseline methods in PyTorch. For training and testing, we used NVIDIA GeForce GTX 1080 Ti with 11GB GPU memory. We minimize the loss of each method via Adam optimizer, for which we searched for the optimal learning rate within the range between  $5 \cdot 10^{-5}$  and  $4 \cdot 10^{-5}$  and weight decay within the range between  $1 \cdot 10^{-4}$  and  $1 \cdot 10^{-2}$ . We trained all methods for max. 30,000 training steps with a batch size of 2048 (except AdvSKM with a batch size of 1024 to fit into GPU). We applied early stopping based on the method performance on validation set without the labels from the target domain. To report the test performance of each method with the error bars, we repeated each experiment with 10 different random seeds (i. e., 10 different random initializations). To compare the runtimes of each method, we report their average



runtimes per 100 training steps since the total runtime (i. e., total number of training steps) varies with the step of early stopping applied at each run. For each method, the average runtimes (per 100 training steps) are the following: 44.83 seconds for **w/o UDA**, 122.81 seconds for **VRADA**, 81.06 seconds for **CoDATS**, 151.20 seconds for **TS-SASA**, 73.67 seconds for **AdvSKM** with a half batch size, 83.93 seconds for CDAN, and 96.11 seconds for our CLUDA.

### Augmentations

To capture the semantic information of medical time series, we apply semantic-preserving augmentations [9, 22, 43] in our CLUDA framework. We list the augmentations and their optimal hyperparameters (search range in parenthesis) below:

**History crop:** We mask out minimum 20 % (10 % – 40 %) of the initial time series with 50 % (20 % – 50 %) probability.

**History cutout:** We mask out random 8-hour time-window (2-hour – 10-hour) of time series with 50 % (20 % – 70 %) probability.

**Channel dropout:** We mask out each channel (i. e., type of measurement) independently with 10 % (5 % – 30 %) probability.

**Gaussian noise:** We apply Gaussian noise to each measurement independently with standard deviation of 0.1 (0.05 – 0.2).

We apply these augmentations sequentially to each medical time series twice. As a result, we have two semantic-preserving augmented views of the same time series for our CLUDA framework. Of note, we trained all the baseline methods with and without the augmentations of time series. We always report the their best results.

## C Prediction Results for AUPRC

The main paper reported the prediction results for the AUROC. Here, we provide the results for AUPRC. Table 9 shows the decompensation prediction results for AUPRC metric. Table 10 shows the in-hospital mortality prediction results for AUPRC metric.

Table 9: Decompensation prediction. Shown: AUPRC (*mean*  $\pm$  *std*) over 10 random initializations.

Source	MIMIC		AUMC	
Target	MIMIC	AUMC	AUMC	MIMIC
w/o UDA	0.240 $\pm$ 0.003	0.208 $\pm$ 0.003	0.214 $\pm$ 0.005	0.198 $\pm$ 0.004
VRADA[31]	0.226 $\pm$ 0.003	0.209 $\pm$ 0.003	0.207 $\pm$ 0.002	0.184 $\pm$ 0.003
CoDATS[40]	0.242 $\pm$ 0.003	0.213 $\pm$ 0.002	0.227 $\pm$ 0.002	0.211 $\pm$ 0.002
AdvSKM[24]	0.243 $\pm$ 0.002	0.215 $\pm$ 0.001	0.230 $\pm$ 0.005	0.214 $\pm$ 0.002
CDAN[25]	0.240 $\pm$ 0.002	0.209 $\pm$ 0.002	0.231 $\pm$ 0.002	<b>0.217 <math>\pm</math> 0.003</b>
CLUDA (ours)	<b>0.253 <math>\pm</math> 0.003</b>	<b>0.223 <math>\pm</math> 0.003</b>	<b>0.239 <math>\pm</math> 0.001</b>	0.215 $\pm$ 0.002

Higher is better. Best value in bold. Black font: main results for UDA. Gray font: source  $\mapsto$  source.

Table 10: In-hospital mortality prediction. Shown: AUPRC (*mean*  $\pm$  *std*) over 10 random initializations.

Source	MIMIC		AUMC	
Target	MIMIC	AUMC	AUMC	MIMIC
w/o UDA	0.513 $\pm$ 0.004	0.412 $\pm$ 0.003	0.430 $\pm$ 0.002	0.427 $\pm$ 0.006
VRADA[31]	0.501 $\pm$ 0.003	0.419 $\pm$ 0.003	0.422 $\pm$ 0.005	0.423 $\pm$ 0.006
CoDATS[40]	0.518 $\pm$ 0.004	0.415 $\pm$ 0.002	0.435 $\pm$ 0.004	0.441 $\pm$ 0.004
AdvSKM[24]	0.518 $\pm$ 0.001	0.421 $\pm$ 0.001	0.441 $\pm$ 0.004	0.443 $\pm$ 0.004
CDAN[25]	0.519 $\pm$ 0.001	0.422 $\pm$ 0.002	0.430 $\pm$ 0.001	0.435 $\pm$ 0.004
CLUDA (ours)	<b>0.522 <math>\pm</math> 0.002</b>	<b>0.428 <math>\pm</math> 0.002</b>	<b>0.446 <math>\pm</math> 0.003</b>	<b>0.452 <math>\pm</math> 0.003</b>

Higher is better. Best value in bold. Black font: main results for UDA. Gray font: source  $\mapsto$  source.

The results confirm our findings from the main paper: overall, our CLUDA achieves the best performance in both source and target domains.

## D Ablation Study (Additional Results)

Here, we provide additional results for our ablation study. Specifically, Table 11 evaluates the decompensation prediction (source: AUMC). Table 12 (source: MIMIC) and Table 13 (source: AUMC) evaluate the in-hospital mortality prediction. Table 14 (source: MIMIC) and Table 15 (source: AUMC) evaluate the length of stay prediction.

Table 11: Ablation study for decompensation prediction. Shown: AUROC (*mean*  $\pm$  *std*) over 10 random initializations.

Source	AUMC	
Target	AUMC	MIMIC
w/o UDA	0.813 $\pm$ 0.005	0.745 $\pm$ 0.004
w/o CL and w/o NNCL ( $\lambda_{CL} = 0, \lambda_{NNCL} = 0$ )	0.818 $\pm$ 0.005	0.761 $\pm$ 0.003
w/o CL ( $\lambda_{CL} = 0$ )	0.822 $\pm$ 0.004	0.763 $\pm$ 0.003
w/o NNCL ( $\lambda_{NNCL} = 0$ )	0.827 $\pm$ 0.001	0.771 $\pm$ 0.004
w/o Discriminator ( $\lambda_{disc} = 0$ )	<b>0.832 <math>\pm</math> 0.002</b>	0.771 $\pm$ 0.002
CLUDA (ours)	0.825 $\pm$ 0.001	<b>0.774 <math>\pm</math> 0.002</b>

Higher is better. Best value in bold. Black font: main results for UDA. Gray font: source  $\mapsto$  source.

Table 12: Ablation study for mortality prediction. Shown: AUROC (*mean*  $\pm$  *std*) over 10 random initializations.

Source	MIMIC	
Target	MIMIC	AUMC
w/o UDA	0.831 $\pm$ 0.001	0.709 $\pm$ 0.002
w/o CL and w/o NNCL ( $\lambda_{CL} = 0, \lambda_{NNCL} = 0$ )	0.830 $\pm$ 0.002	0.709 $\pm$ 0.004
w/o CL ( $\lambda_{CL} = 0$ )	0.836 $\pm$ 0.001	0.730 $\pm$ 0.003
w/o NNCL ( $\lambda_{NNCL} = 0$ )	0.840 $\pm$ 0.002	0.721 $\pm$ 0.004
w/o Discriminator ( $\lambda_{disc} = 0$ )	<b>0.842 <math>\pm</math> 0.002</b>	<b>0.747 <math>\pm</math> 0.004</b>
CLUDA (ours)	0.836 $\pm$ 0.001	0.739 $\pm$ 0.004

Higher is better. Best value in bold. Black font: main results for UDA. Gray font: source  $\mapsto$  source.

Table 13: Ablation study for mortality prediction. Shown: AUROC (*mean*  $\pm$  *std*) over 10 random initializations.

Source	AUMC	
Target	AUMC	MIMIC
w/o UDA	0.721 $\pm$ 0.005	0.774 $\pm$ 0.006
w/o CL and w/o NNCL ( $\lambda_{CL} = 0, \lambda_{NNCL} = 0$ )	0.724 $\pm$ 0.004	0.778 $\pm$ 0.004
w/o CL ( $\lambda_{CL} = 0$ )	0.743 $\pm$ 0.001	0.781 $\pm$ 0.003
w/o NNCL ( $\lambda_{NNCL} = 0$ )	0.746 $\pm$ 0.004	0.781 $\pm$ 0.003
w/o Discriminator ( $\lambda_{disc} = 0$ )	0.749 $\pm$ 0.002	0.784 $\pm$ 0.004
CLUDA (ours)	<b>0.750 <math>\pm</math> 0.001</b>	<b>0.789 <math>\pm</math> 0.002</b>

Higher is better. Best value in bold. Black font: main results for UDA. Gray font: source  $\mapsto$  source.

Overall, the ablation study with different variants of our CLUDA confirms the importance of each component in our framework. Specifically, our CLUDA improves the prediction performance over all of its variants in all tasks except one (in-hospital mortality prediction from MIMIC to AUMC). For this task, it is important to note that the best performing variant is w/o Discriminator, which has all the novel components of our CLUDA framework.

Table 14: Ablation study for length of stay prediction. Shown: KAPPA (*mean*  $\pm$  *std*) over 10 random initializations.

Source	MIMIC	
Target	MIMIC	AUMC
w/o UDA	0.178 $\pm$ 0.002	0.169 $\pm$ 0.003
w/o CL and w/o NNCL ( $\lambda_{CL} = 0, \lambda_{NNCL} = 0$ )	0.173 $\pm$ 0.002	0.160 $\pm$ 0.005
w/o CL ( $\lambda_{CL} = 0$ )	0.212 $\pm$ 0.001	0.194 $\pm$ 0.009
w/o NNCL ( $\lambda_{NNCL} = 0$ )	0.212 $\pm$ 0.002	0.155 $\pm$ 0.003
w/o Discriminator ( $\lambda_{disc} = 0$ )	0.214 $\pm$ 0.001	0.196 $\pm$ 0.002
CLUDA (ours)	<b>0.216 <math>\pm</math> 0.001</b>	<b>0.202 <math>\pm</math> 0.006</b>

Higher is better. Best value in bold. Black font: main results for UDA. Gray font: source  $\mapsto$  source.

Table 15: Ablation study for length of stay prediction. Shown: KAPPA (*mean*  $\pm$  *std*) over 10 random initializations.

Source	AUMC	
Target	AUMC	MIMIC
w/o UDA	0.246 $\pm$ 0.001	0.122 $\pm$ 0.001
w/o CL and w/o NNCL ( $\lambda_{CL} = 0, \lambda_{NNCL} = 0$ )	0.242 $\pm$ 0.002	0.120 $\pm$ 0.003
w/o CL ( $\lambda_{CL} = 0$ )	0.271 $\pm$ 0.002	0.122 $\pm$ 0.003
w/o NNCL ( $\lambda_{NNCL} = 0$ )	0.274 $\pm$ 0.001	0.113 $\pm$ 0.001
w/o Discriminator ( $\lambda_{disc} = 0$ )	0.274 $\pm$ 0.001	0.125 $\pm$ 0.004
CLUDA (ours)	<b>0.276 <math>\pm</math> 0.002</b>	<b>0.129 <math>\pm</math> 0.003</b>

Higher is better. Best value in bold. Black font: main results for UDA. Gray font: source  $\mapsto$  source.

## E Unsupervised Domain Adaptation across Various Age Groups

Following the earlier works [31, 4], we conducted additional experiments to compare the UDA performance of our CLUDA framework across various age groups. We consider the following groups: (1) Group 1: working-age adult (20 to 45 years old patients); (2) Group 2: old working-age adult (46 to 65 years old patients); (3) Group 3: elderly (66 to 85 years old patients); and (4) Group 4: seniors (85+ years old patients). Therefore, within each dataset (MIMIC and AUMC), we list the results of all combinations of Source  $\mapsto$  Target for in-hospital mortality prediction (i. e., Group 1  $\mapsto$  Group 2, Group 1  $\mapsto$  Group 3,  $\dots$ , Group 4  $\mapsto$  Group 3). Results are shown in Table 16 for MIMIC and Table 17 for AUMC.

We further extend the experiments to **across datasets**. That means, we pick the source domain as one age group from one dataset (e. g., Group 1 of MIMIC) and pick the target domain as one age group from the other dataset (e. g., Group 3 of AUMC). We, again, conducted the experiments for all combinations of age groups across the datasets. Results are shown in Table 18 from MIMIC to AUMC and Table 19 from AUMC to MIMIC.

Table 16: In-hospital mortality prediction between various age groups of MIMIC. Shown: AUROC (*mean  $\pm$  std*) over 10 random initializations.

Sour $\mapsto$ Tar	w/o UDA	VRADA[31]	CoDATS[40]	AdvSKM[24]	CDAN[25]	CLUDA (ours)
1 $\mapsto$ 2	0.744 $\pm$ 0.002	0.786 $\pm$ 0.002	0.744 $\pm$ 0.002	0.757 $\pm$ 0.005	0.726 $\pm$ 0.005	<b>0.798 <math>\pm</math> 0.003</b>
1 $\mapsto$ 3	0.685 $\pm$ 0.003	0.729 $\pm$ 0.003	0.685 $\pm$ 0.004	0.702 $\pm$ 0.008	0.674 $\pm$ 0.008	<b>0.747 <math>\pm</math> 0.004</b>
1 $\mapsto$ 4	0.617 $\pm$ 0.007	0.631 $\pm$ 0.004	0.616 $\pm$ 0.006	0.619 $\pm$ 0.004	0.612 $\pm$ 0.007	<b>0.649 <math>\pm</math> 0.007</b>
2 $\mapsto$ 1	0.818 $\pm$ 0.007	0.828 $\pm$ 0.006	0.822 $\pm$ 0.007	0.835 $\pm$ 0.001	0.842 $\pm$ 0.001	<b>0.856 <math>\pm</math> 0.002</b>
2 $\mapsto$ 3	0.790 $\pm$ 0.004	0.746 $\pm$ 0.006	<b>0.797 <math>\pm</math> 0.004</b>	0.792 $\pm$ 0.003	0.788 $\pm$ 0.001	0.796 $\pm$ 0.002
2 $\mapsto$ 4	0.696 $\pm$ 0.003	0.649 $\pm$ 0.003	<b>0.699 <math>\pm</math> 0.003</b>	0.696 $\pm$ 0.004	0.681 $\pm$ 0.006	0.697 $\pm$ 0.006
3 $\mapsto$ 1	0.787 $\pm$ 0.005	0.808 $\pm$ 0.003	0.788 $\pm$ 0.006	0.798 $\pm$ 0.003	0.789 $\pm$ 0.005	<b>0.822 <math>\pm</math> 0.007</b>
3 $\mapsto$ 2	0.833 $\pm$ 0.002	0.805 $\pm$ 0.007	0.832 $\pm$ 0.004	0.835 $\pm$ 0.001	0.777 $\pm$ 0.001	<b>0.843 <math>\pm</math> 0.002</b>
3 $\mapsto$ 4	<b>0.751 <math>\pm</math> 0.003</b>	0.684 $\pm$ 0.002	0.748 $\pm$ 0.004	0.745 $\pm$ 0.005	0.689 $\pm$ 0.004	0.745 $\pm$ 0.010
4 $\mapsto$ 1	0.783 $\pm$ 0.005	0.790 $\pm$ 0.008	0.783 $\pm$ 0.006	0.788 $\pm$ 0.005	0.785 $\pm$ 0.008	<b>0.807 <math>\pm</math> 0.022</b>
4 $\mapsto$ 2	0.761 $\pm$ 0.005	0.760 $\pm$ 0.004	0.762 $\pm$ 0.004	0.765 $\pm$ 0.004	0.758 $\pm$ 0.007	<b>0.769 <math>\pm</math> 0.012</b>
4 $\mapsto$ 3	0.736 $\pm$ 0.006	0.723 $\pm$ 0.006	0.737 $\pm$ 0.007	0.734 $\pm$ 0.004	0.730 $\pm$ 0.005	<b>0.748 <math>\pm</math> 0.009</b>

Higher is better. Best value in bold.

Table 17: In-hospital mortality prediction between various age groups of AUMC. Shown: AUROC (*mean  $\pm$  std*) over 10 random initializations.

Sour $\mapsto$ Tar	w/o UDA	VRADA[31]	CoDATS[40]	AdvSKM[24]	CDAN[25]	CLUDA (ours)
1 $\mapsto$ 2	0.557 $\pm$ 0.008	<b>0.583 <math>\pm</math> 0.005</b>	0.545 $\pm$ 0.006	0.562 $\pm$ 0.006	0.551 $\pm$ 0.007	0.571 $\pm$ 0.007
1 $\mapsto$ 3	0.602 $\pm$ 0.008	0.659 $\pm$ 0.008	0.602 $\pm$ 0.005	0.623 $\pm$ 0.007	0.578 $\pm$ 0.005	<b>0.686 <math>\pm</math> 0.005</b>
1 $\mapsto$ 4	0.683 $\pm$ 0.007	0.732 $\pm$ 0.009	0.672 $\pm$ 0.010	0.702 $\pm$ 0.004	0.677 $\pm$ 0.008	<b>0.749 <math>\pm</math> 0.006</b>
2 $\mapsto$ 1	0.719 $\pm$ 0.008	0.716 $\pm$ 0.007	0.728 $\pm$ 0.006	0.740 $\pm$ 0.007	0.688 $\pm$ 0.004	<b>0.743 <math>\pm</math> 0.004</b>
2 $\mapsto$ 3	0.728 $\pm$ 0.009	0.743 $\pm$ 0.008	0.728 $\pm$ 0.008	0.740 $\pm$ 0.010	0.726 $\pm$ 0.008	<b>0.765 <math>\pm</math> 0.008</b>
2 $\mapsto$ 4	0.795 $\pm$ 0.006	0.783 $\pm$ 0.009	0.798 $\pm$ 0.003	<b>0.800 <math>\pm</math> 0.006</b>	0.762 $\pm$ 0.006	0.795 $\pm$ 0.006
3 $\mapsto$ 1	0.780 $\pm$ 0.008	0.761 $\pm$ 0.008	0.778 $\pm$ 0.009	0.781 $\pm$ 0.010	0.766 $\pm$ 0.005	<b>0.812 <math>\pm</math> 0.009</b>
3 $\mapsto$ 2	0.595 $\pm$ 0.002	0.618 $\pm$ 0.006	0.588 $\pm$ 0.009	0.604 $\pm$ 0.004	0.647 $\pm$ 0.008	<b>0.657 <math>\pm</math> 0.012</b>
3 $\mapsto$ 4	0.817 $\pm$ 0.005	0.788 $\pm$ 0.013	0.815 $\pm$ 0.006	0.832 $\pm$ 0.003	0.790 $\pm$ 0.006	<b>0.836 <math>\pm</math> 0.006</b>
4 $\mapsto$ 1	0.730 $\pm$ 0.007	<b>0.739 <math>\pm</math> 0.006</b>	0.727 $\pm$ 0.009	0.738 $\pm$ 0.006	0.721 $\pm$ 0.005	0.731 $\pm$ 0.007
4 $\mapsto$ 2	0.640 $\pm$ 0.007	0.618 $\pm$ 0.008	0.640 $\pm$ 0.004	0.628 $\pm$ 0.010	<b>0.669 <math>\pm</math> 0.009</b>	0.658 $\pm$ 0.007
4 $\mapsto$ 3	0.709 $\pm$ 0.011	0.715 $\pm$ 0.009	0.708 $\pm$ 0.010	0.717 $\pm$ 0.002	0.707 $\pm$ 0.004	<b>0.740 <math>\pm</math> 0.006</b>

Higher is better. Best value in bold.

Overall, in this section we present 56 prediction tasks to compare the methods across various age groups in both datasets. Out of 56 tasks, our CLUDA achieves the best performance 38 of them, significantly outperforming the other methods. In comparison, the best baseline method AdvSKM achieves the best result in only 6 out of 56 tasks. This highlights the consistent performance of our CLUDA in various domains.

Table 18: In-hospital mortality prediction between various age groups from MIMIC to AUMC.  
Shown: AUROC (*mean*  $\pm$  *std*) over 10 random initializations.

Sour $\mapsto$ Tar	w/o UDA	VRADA[31]	CoDATS[40]	AdvSKM[24]	CDAN[25]	CLUDA (ours)
1 $\mapsto$ 1	0.736 $\pm$ 0.007	0.751 $\pm$ 0.008	0.731 $\pm$ 0.004	0.734 $\pm$ 0.005	0.754 $\pm$ 0.010	<b>0.782</b> $\pm$ <b>0.008</b>
1 $\mapsto$ 2	0.628 $\pm$ 0.001	0.721 $\pm$ 0.005	0.627 $\pm$ 0.002	0.637 $\pm$ 0.002	0.614 $\pm$ 0.005	<b>0.731</b> $\pm$ <b>0.003</b>
1 $\mapsto$ 3	0.662 $\pm$ 0.001	0.688 $\pm$ 0.010	0.657 $\pm$ 0.003	0.671 $\pm$ 0.003	0.654 $\pm$ 0.006	<b>0.707</b> $\pm$ <b>0.003</b>
1 $\mapsto$ 4	0.754 $\pm$ 0.004	0.745 $\pm$ 0.009	0.753 $\pm$ 0.007	0.753 $\pm$ 0.004	0.745 $\pm$ 0.004	0.754 $\pm$ 0.005
2 $\mapsto$ 1	<b>0.835</b> $\pm$ <b>0.005</b>	0.760 $\pm$ 0.007	0.828 $\pm$ 0.006	0.832 $\pm$ 0.001	0.783 $\pm$ 0.007	0.822 $\pm$ 0.002
2 $\mapsto$ 2	0.629 $\pm$ 0.006	0.699 $\pm$ 0.007	0.633 $\pm$ 0.009	0.635 $\pm$ 0.001	0.691 $\pm$ 0.006	<b>0.705</b> $\pm$ <b>0.003</b>
2 $\mapsto$ 3	0.656 $\pm$ 0.005	0.701 $\pm$ 0.004	0.667 $\pm$ 0.007	0.689 $\pm$ 0.002	0.665 $\pm$ 0.007	<b>0.714</b> $\pm$ <b>0.004</b>
2 $\mapsto$ 4	0.773 $\pm$ 0.006	0.764 $\pm$ 0.007	0.776 $\pm$ 0.005	0.777 $\pm$ 0.005	0.755 $\pm$ 0.007	<b>0.807</b> $\pm$ <b>0.007</b>
3 $\mapsto$ 1	0.763 $\pm$ 0.005	0.748 $\pm$ 0.007	0.754 $\pm$ 0.007	0.776 $\pm$ 0.008	0.746 $\pm$ 0.006	<b>0.789</b> $\pm$ <b>0.006</b>
3 $\mapsto$ 2	0.627 $\pm$ 0.011	0.622 $\pm$ 0.006	0.615 $\pm$ 0.008	0.621 $\pm$ 0.003	0.672 $\pm$ 0.008	<b>0.691</b> $\pm$ <b>0.006</b>
3 $\mapsto$ 3	0.711 $\pm$ 0.007	0.701 $\pm$ 0.007	0.712 $\pm$ 0.006	0.716 $\pm$ 0.003	0.702 $\pm$ 0.007	<b>0.751</b> $\pm$ <b>0.005</b>
3 $\mapsto$ 4	0.782 $\pm$ 0.008	0.750 $\pm$ 0.006	0.784 $\pm$ 0.007	0.785 $\pm$ 0.005	0.756 $\pm$ 0.007	<b>0.796</b> $\pm$ <b>0.008</b>
4 $\mapsto$ 1	0.714 $\pm$ 0.004	0.676 $\pm$ 0.006	0.697 $\pm$ 0.006	<b>0.716</b> $\pm$ <b>0.004</b>	0.689 $\pm$ 0.007	0.689 $\pm$ 0.006
4 $\mapsto$ 2	0.668 $\pm$ 0.007	0.666 $\pm$ 0.006	0.661 $\pm$ 0.007	0.649 $\pm$ 0.006	<b>0.713</b> $\pm$ <b>0.009</b>	0.673 $\pm$ 0.005
4 $\mapsto$ 3	0.619 $\pm$ 0.002	0.627 $\pm$ 0.008	0.614 $\pm$ 0.001	0.606 $\pm$ 0.002	0.620 $\pm$ 0.008	<b>0.635</b> $\pm$ <b>0.005</b>
4 $\mapsto$ 4	0.758 $\pm$ 0.001	0.709 $\pm$ 0.008	0.757 $\pm$ 0.001	0.744 $\pm$ 0.009	0.748 $\pm$ 0.003	<b>0.768</b> $\pm$ <b>0.004</b>

Higher is better. Best value in bold.

Table 19: In-hospital mortality prediction between various age groups from AUMC to MIMIC.  
Shown: AUROC (*mean*  $\pm$  *std*) over 10 random initializations.

Sour $\mapsto$ Tar	w/o UDA	VRADA[31]	CoDATS[40]	AdvSKM[24]	CDAN[25]	CLUDA (ours)
1 $\mapsto$ 1	0.693 $\pm$ 0.004	0.733 $\pm$ 0.007	0.694 $\pm$ 0.003	0.698 $\pm$ 0.007	0.681 $\pm$ 0.009	<b>0.791</b> $\pm$ <b>0.005</b>
1 $\mapsto$ 2	0.665 $\pm$ 0.008	0.722 $\pm$ 0.006	0.666 $\pm$ 0.007	0.696 $\pm$ 0.004	0.648 $\pm$ 0.003	<b>0.776</b> $\pm$ <b>0.004</b>
1 $\mapsto$ 3	0.609 $\pm$ 0.009	0.644 $\pm$ 0.010	0.609 $\pm$ 0.007	0.625 $\pm$ 0.006	0.594 $\pm$ 0.008	<b>0.679</b> $\pm$ <b>0.003</b>
1 $\mapsto$ 4	0.600 $\pm$ 0.003	0.579 $\pm$ 0.007	0.599 $\pm$ 0.004	<b>0.609</b> $\pm$ <b>0.006</b>	0.585 $\pm$ 0.009	0.598 $\pm$ 0.005
2 $\mapsto$ 1	0.703 $\pm$ 0.008	0.747 $\pm$ 0.004	0.735 $\pm$ 0.007	0.727 $\pm$ 0.006	0.736 $\pm$ 0.014	<b>0.780</b> $\pm$ <b>0.009</b>
2 $\mapsto$ 2	0.684 $\pm$ 0.007	0.758 $\pm$ 0.008	0.697 $\pm$ 0.005	0.730 $\pm$ 0.010	0.757 $\pm$ 0.004	<b>0.771</b> $\pm$ <b>0.003</b>
2 $\mapsto$ 3	0.641 $\pm$ 0.016	0.693 $\pm$ 0.006	0.648 $\pm$ 0.011	0.659 $\pm$ 0.006	0.677 $\pm$ 0.002	<b>0.702</b> $\pm$ <b>0.007</b>
2 $\mapsto$ 4	0.592 $\pm$ 0.005	0.590 $\pm$ 0.011	0.597 $\pm$ 0.005	0.573 $\pm$ 0.001	0.556 $\pm$ 0.006	<b>0.608</b> $\pm$ <b>0.002</b>
3 $\mapsto$ 1	<b>0.805</b> $\pm$ <b>0.007</b>	0.784 $\pm$ 0.010	0.794 $\pm$ 0.009	0.801 $\pm$ 0.005	0.778 $\pm$ 0.005	0.785 $\pm$ 0.009
3 $\mapsto$ 2	0.751 $\pm$ 0.008	0.769 $\pm$ 0.006	0.747 $\pm$ 0.007	0.747 $\pm$ 0.007	0.698 $\pm$ 0.006	<b>0.774</b> $\pm$ <b>0.010</b>
3 $\mapsto$ 3	0.720 $\pm$ 0.010	0.723 $\pm$ 0.006	0.718 $\pm$ 0.006	0.722 $\pm$ 0.007	0.714 $\pm$ 0.004	<b>0.729</b> $\pm$ <b>0.005</b>
3 $\mapsto$ 4	0.622 $\pm$ 0.007	0.608 $\pm$ 0.008	0.615 $\pm$ 0.010	<b>0.624</b> $\pm$ <b>0.003</b>	0.598 $\pm$ 0.009	0.615 $\pm$ 0.003
4 $\mapsto$ 1	0.801 $\pm$ 0.008	0.756 $\pm$ 0.008	0.808 $\pm$ 0.005	0.819 $\pm$ 0.003	0.786 $\pm$ 0.005	0.819 $\pm$ 0.005
4 $\mapsto$ 2	0.750 $\pm$ 0.016	0.739 $\pm$ 0.007	0.756 $\pm$ 0.007	<b>0.761</b> $\pm$ <b>0.008</b>	0.744 $\pm$ 0.003	0.752 $\pm$ 0.004
4 $\mapsto$ 3	0.709 $\pm$ 0.007	0.695 $\pm$ 0.004	0.710 $\pm$ 0.008	0.711 $\pm$ 0.004	0.697 $\pm$ 0.002	0.711 $\pm$ 0.003
4 $\mapsto$ 4	0.697 $\pm$ 0.006	0.664 $\pm$ 0.008	0.695 $\pm$ 0.007	<b>0.698</b> $\pm$ <b>0.003</b>	0.684 $\pm$ 0.005	0.679 $\pm$ 0.005

Higher is better. Best value in bold.

## F CLUDA with SimCLR

In our CLUDA framework, we capture semantic information in time series data by leveraging contrastive learning. Specifically, we adapt momentum contrast (MoCo) [19] for contrastive learning in our framework. This choice is motivated by earlier research from other domains [19, 8, 43, 11], where MoCo was found to yield more stable negative samples (due to the momentum-updated feature extractor) as compared to other approaches throughout each training step, such as SimCLR[7]. In principle, stability yields stronger negative samples for the contrastive learning objectives and, therefore, increases the mutual information between the positive pair (i. e., two augmented views of the same sample). Furthermore, MoCo allows storing the negative samples within a queue, facilitating a larger number of negative samples for the contrastive loss as compared to SimCLR. As shown earlier [1, 36, 37], the lower bound of the mutual information between the positive pair increases with a larger number of negative samples in CL. With that motivation, we opted for MoCo [19] in our CLUDA instead of SimCLR[7]. Nevertheless, we evaluate our choice through numerical experiments below.

We now further perform an ablation study where we repeat the experiments with SimCLR (instead of MoCo). Specifically, we provide results for decompensation prediction (see Table 20), in-hospital mortality prediction (see Table 21), and length of stay prediction (see Table 22).

Table 20: Decompensation prediction. Shown: AUROC (*mean*  $\pm$  *std*) over 10 random initializations.

Source	MIMIC		AUMC	
Target	MIMIC	AUMC	AUMC	MIMIC
w/o UDA	0.831 $\pm$ 0.001	0.771 $\pm$ 0.004	0.813 $\pm$ 0.005	0.745 $\pm$ 0.004
CLUDA w/ SimCLR	0.826 $\pm$ 0.001	0.776 $\pm$ 0.001	0.801 $\pm$ 0.005	0.751 $\pm$ 0.005
CLUDA (ours)	0.832 $\pm$ 0.002	<b>0.791 <math>\pm</math> 0.004</b>	<b>0.825 <math>\pm</math> 0.001</b>	<b>0.774 <math>\pm</math> 0.002</b>

Higher is better. Best value in bold. Black font: main results for UDA. Gray font: source  $\mapsto$  source.

Table 21: In-hospital mortality prediction. Shown: AUROC (*mean*  $\pm$  *std*) over 10 random initializations.

Source	MIMIC		AUMC	
Target	MIMIC	AUMC	AUMC	MIMIC
w/o UDA	0.831 $\pm$ 0.001	0.709 $\pm$ 0.002	0.721 $\pm$ 0.005	0.774 $\pm$ 0.006
CLUDA w/ SimCLR	0.827 $\pm$ 0.001	0.724 $\pm$ 0.004	0.748 $\pm$ 0.002	0.781 $\pm$ 0.002
CLUDA (ours)	<b>0.836 <math>\pm</math> 0.001</b>	<b>0.739 <math>\pm</math> 0.004</b>	<b>0.750 <math>\pm</math> 0.001</b>	<b>0.789 <math>\pm</math> 0.002</b>

Higher is better. Best value in bold. Black font: main results for UDA. Gray font: source  $\mapsto$  source.

Table 22: Length of stay prediction. Shown: KAPPA (*mean*  $\pm$  *std*) over 10 random initializations.

Source	MIMIC		AUMC	
Target	MIMIC	AUMC	AUMC	MIMIC
w/o UDA	0.178 $\pm$ 0.002	0.169 $\pm$ 0.003	0.246 $\pm$ 0.001	0.122 $\pm$ 0.001
CLUDA w/ SimCLR	0.203 $\pm$ 0.001	0.178 $\pm$ 0.006	0.258 $\pm$ 0.005	0.107 $\pm$ 0.003
CLUDA (ours)	<b>0.216 <math>\pm</math> 0.001</b>	<b>0.202 <math>\pm</math> 0.006</b>	<b>0.276 <math>\pm</math> 0.002</b>	<b>0.129 <math>\pm</math> 0.003</b>

Higher is better. Best value in bold. Black font: main results for UDA. Gray font: source  $\mapsto$  source.

The results confirm our choice for MoCo instead of SimCLR in capturing the semantic information in time series. Specifically, our CLUDA improves the result of CLUDA w/ SimCLR in all tasks by a large margin. Despite being inferior to our CLUDA, CLUDA w/ SimCLR achieves better UDA performance compared to other baseline methods in decompensation prediction from MIMIC

to AUMC, in-hospital mortality prediction from AUMC to MIMIC, and length of stay prediction from MIMIC to AUMC. This shows the importance of leveraging the semantic information into unsupervised domain adaptation. Besides, it highlights that our CLUDA can be further improved in the future with the recent advances in capturing the semantic information of time series.